Interim Report: Fabrication and Structural Testing of the Second RTM Carbon Fiber Composite End Plate

Subcontractor Report
prepared by

D·R Technologies, Inc.

San Diego, CA

October 1998

IAT.R 0189

Institute for Advanced Technology
The University of Texas at Austin

IAT

REPORT DOCUMENTATION PAGE

Form Approved
OMB NO. 0704-0188

1. AGENCY USE ONLY (Leave blank)	2. REPORT DATE	3. REPORT TYPE AND DATES COVERED
	October 1998	Technical Report 1/98-9/98

4. TITLE AND SUBTITLE

Interim Report: Fabrication and Structural Testing of the Second RTM Carbon Fiber Composite End Plate

5. FUNDING NUMBERS

Contract # DAAA21-93-C-0101

6. AUTHOR(S)

D·R Technologies, Inc.

7. PERFORMING ORGANIZATION NAME(S) AND ADDRESS(ES)

Institute for Advanced Technology
The University of Texas at Austin
4030-2 W. Braker Lane, #200
Austin, TX 78759

8. PERFORMING ORGANIZATION REPORT NUMBER

IAT.R 0189

9. SPONSORING / MONITORING AGENCY NAME(S) AND ADDRESS(ES)

U.S. Army Research Laboratory
ATTN: AMSRL-WM-B
Aberdeen Proving Ground, MD 21005-5066

10. SPONSORING / MONITORING AGENCY REPORT NUMBER

11. SUPPLEMENTARY NOTES

The view, opinions and/or findings contained in this report are those of the author(s) and should not be considered as an official Department of the Army position, policy, or decision, unless so designated by other documentation.

12a. DISTRIBUTION / AVAILABILITY STATEMENT

Approved for public release; distribution unlimited.

12b. DISTRIBUTION CODE

A

13. ABSTRACT *(Maximum 200 words)*

In a previous report DR Technologies described the fabrication and testing of the first carbon fiber end plate for the subscale compulsator. The first end plate demonstrated the producibility of the carbon/epoxy composite concept using RTM technology and, following an unintentional overload during structural testing, provided coupon-level material properties. A second identical plate was fabricated in this reporting period, nondestructive structural stiffness measurements were made, and the plate was delivered to UT-CEM for further evaluation. This report summarizes the fabrication, testing, and analysis of the second end plate.

14. SUBJECT TERMS

carbon composite, subscale compulsator, resin transfer, stiffness, tests

15. NUMBER OF PAGES

13

16. PRICE CODE

17. SECURITY CLASSIFICATION OF REPORT	18. SECURITY CLASSIFICATION OF THIS PAGE	19. SECURITY CLASSIFICATION OF ABSTRACT	20. LIMITATION OF ABSTRACT
Unclassified	Unclassified	Unclassified	UL

Table of Contents

List of Figures

List of Figures, Cont'd.

Interim Report: Fabrication and Structural Testing of the Second RTM Carbon Fiber Composite End Plate

D·R Technologies, Inc.

Introduction

In a previous report [1] we described the fabrication and testing of the first carbon fiber end plate for the subscale compulsator. The first end plate demonstrated the producibility of the carbon/epoxy composite concept using RTM technology and, following an unintentional overload during structural testing, provided coupon-level material properties. A second identical plate was fabricated in this reporting period, nondestructive structural stiffness measurements were made, and the plate was delivered to UT-CEM for further evaluation. This report summarizes the fabrication, testing, and analysis of the second end plate.

End Plate Fabrication

The fabrication of the second end plate, shown in Figure 1, was completed in an identical fashion to the first one. There were only a few minor differences designed to simplify the operation. These differences were focused on the ease of assembling the carbon cloth preforms and injecting the resin into the closed mold. For this plate, the alcove preforms were tackified with a spray adhesive to allow easier assembly and to prevent motion of the alcove preforms during mold closure. In addition, the radial edges of the alcove preforms were capped with glass scrim cloth to avoid pinching them between the tool sections. The cross section of the plate through a radial alcove gusset is shown in Figure 2. The resin inlet and outlet ports were positioned 180 degrees from each other to minimize pressure gradients. The tool evacuation and resin injection were done as before, with approximately the same amount of resin injected as for the first plate. The removal of the cured sample was considerably easier than the first plate.

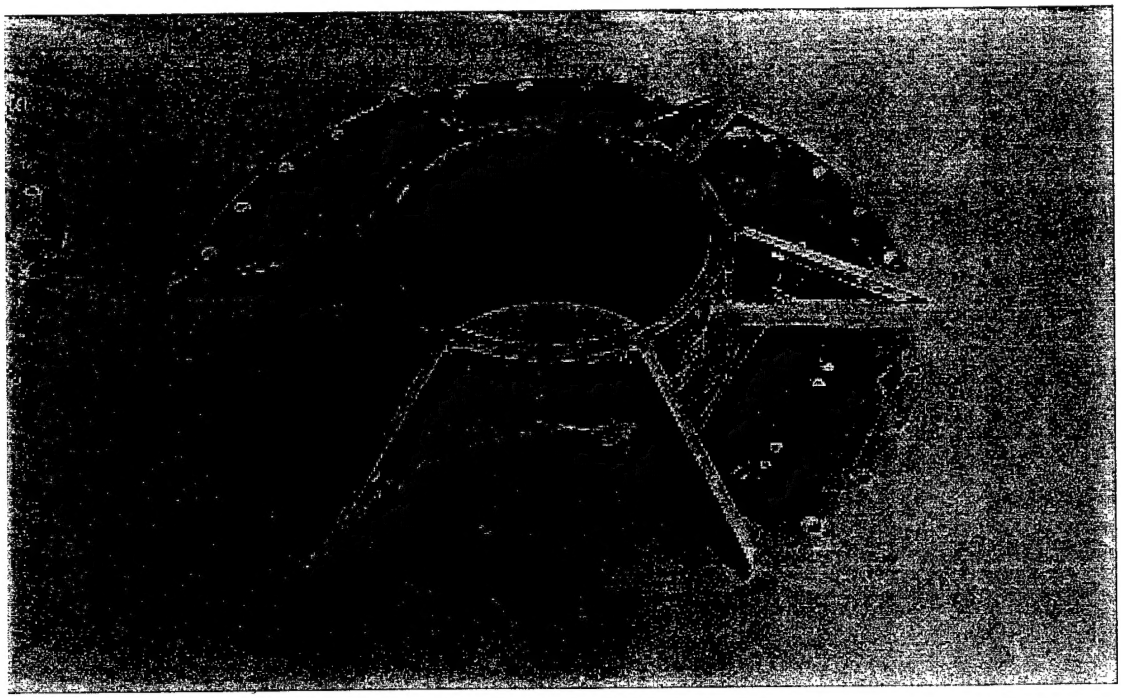

Figure 1. Carbon composite end plate no. 2.

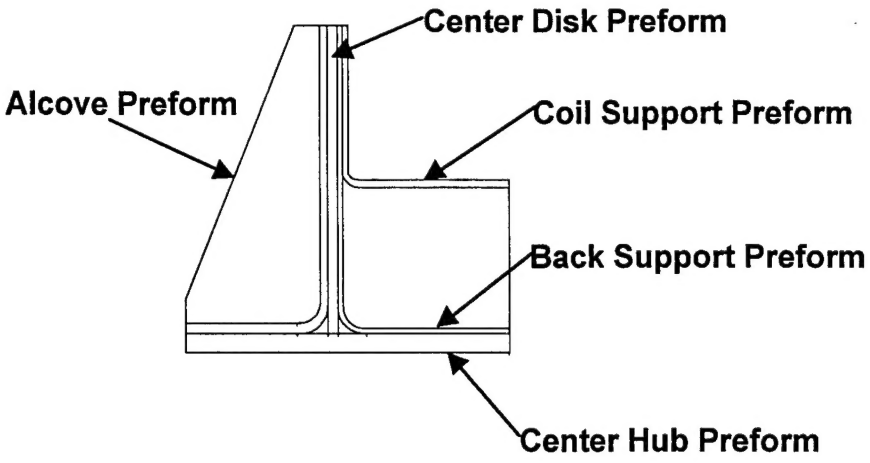

Figure 2. Location of preform sections.

Post-Test Observations and Machining

Visual observation of the finished specimen revealed good composite quality with no visible dry areas or other significant imperfections. The measured dimensions of the cured part are shown in Figure 3. A measurement of the principal dimensions of the plate revealed that the central disk structure was slightly non-planar, with a maximum out of plane warpage of approximately 0.09 inches peak-to-peak, as measured at the disk edge. The plate was machined to bring it to final dimensions on the disk outer diameter and central cylinder inner diameter, and to remove the warpage from the center disk on the side opposite to the alcoves. Also, a set of twenty four (24) 0.672-inch diameter mounting holes were machined into the central disk on a 30.75-inch diameter base circle. Figure 4 shows the final machined dimensions and the mounting holes.

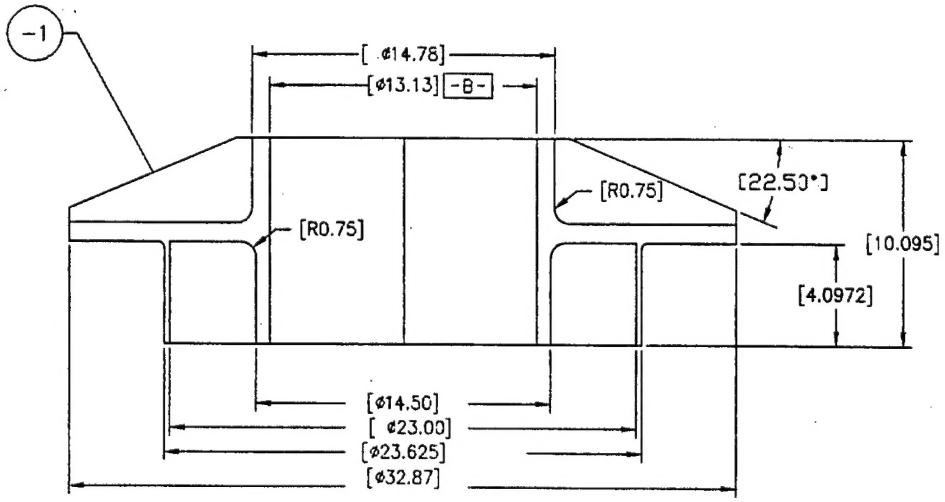

Figure 3. Postcure measured end plate dimensions.

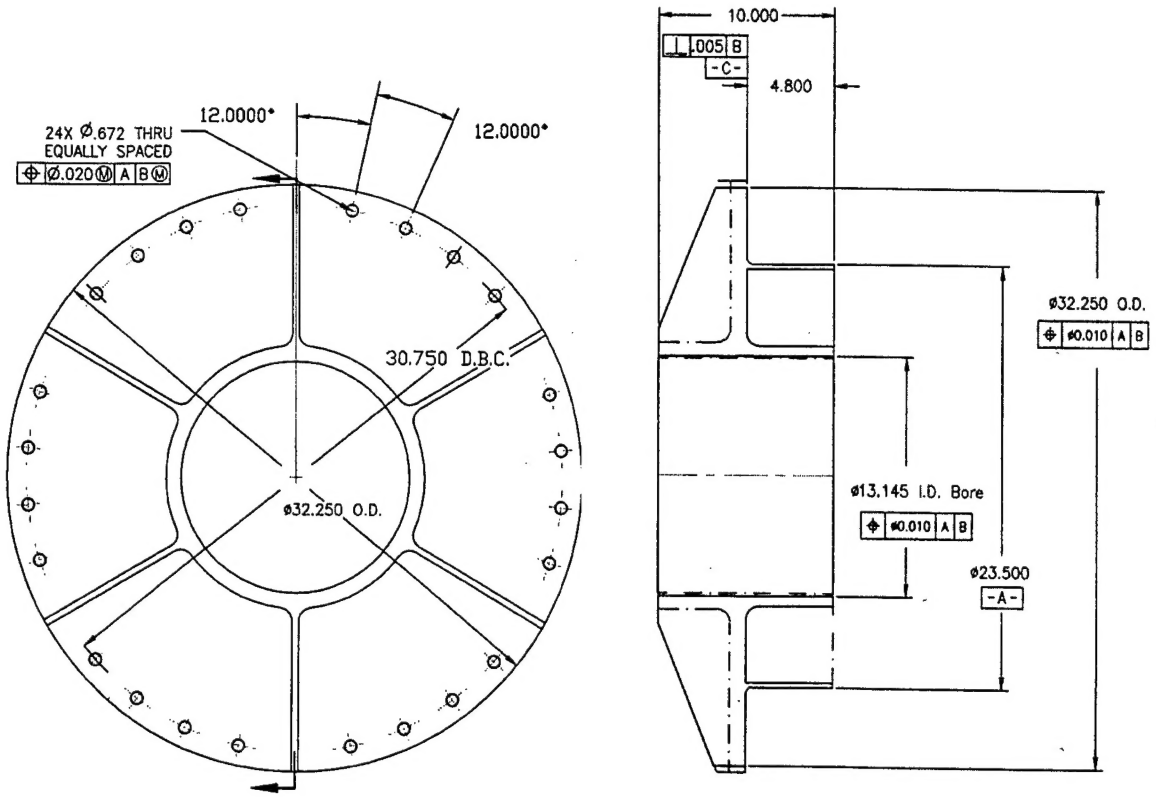

Figure 4. Final machined dimensions for composite end plate no. 2.

Static Testing

The plate was statically tested in a 600,000-lb computer-controlled hydraulic test machine at the University of California, San Diego to determine its bending stiffness. The disk was supported along the edge by circular steel segments, as shown schematically in Figure 5, and in the photograph in Figure 6. The inner radius of the segments was set to coincide with the center of the mounting holes. Therefore the plate could be considered as being simply supported along the bolt hole center diameter. The plate was loaded uniformly along the top edge of the central cylinder, simulating axial loading of the plate under operational conditions. The test setup is shown in Figure 7.

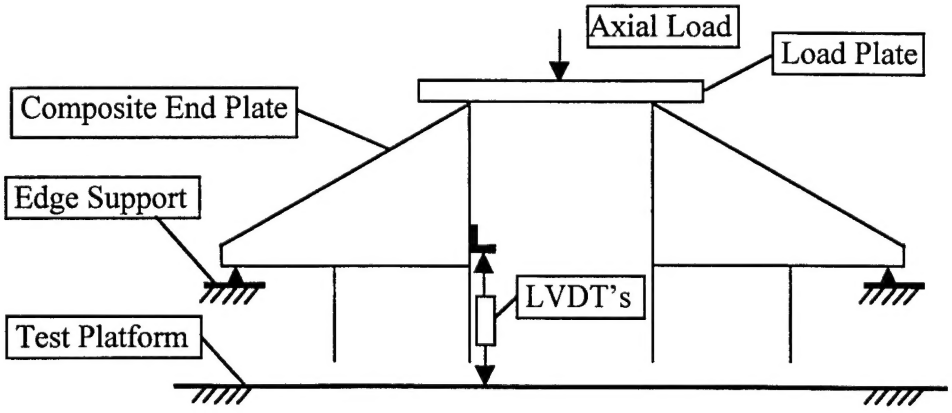

Figure 5. Schematic of test setup and instrumentation for end plate static test.

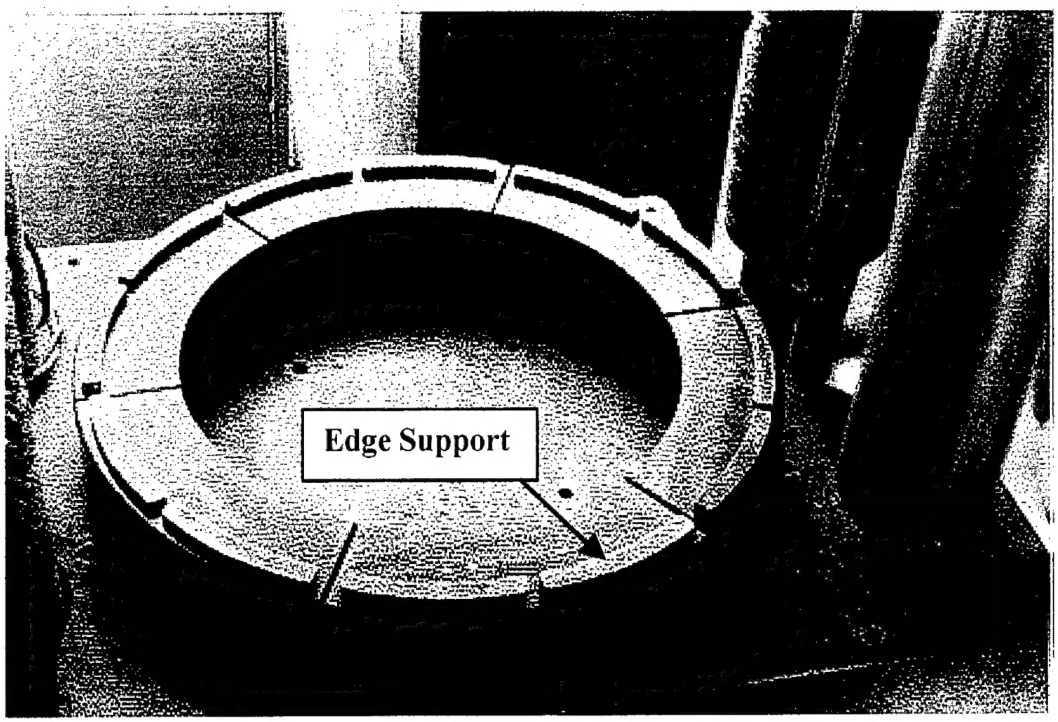

Figure 6. Edge support arrangement for composite end plate structural test.

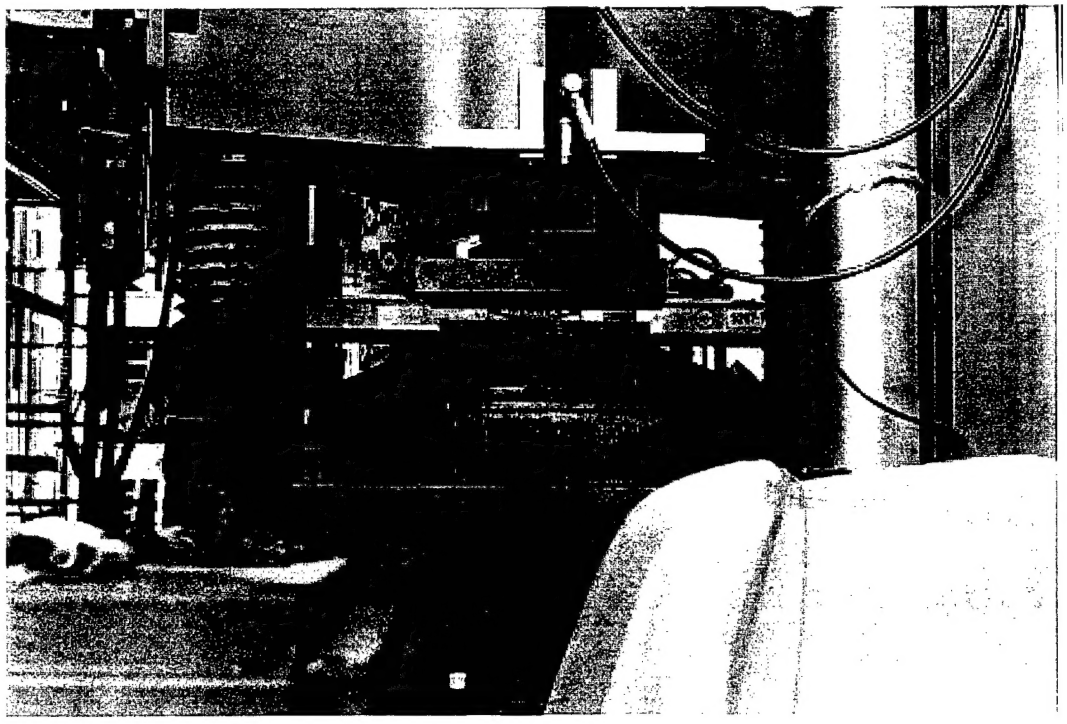

Figure 7. Test setup for composite end plate static test.

The measured quantities were the axial load and the axial displacement of the cylinder at three locations at 120° apart on the inner surface of the cylinder, as indicated by the displacement transducer (LVDT) in Figure 5. The displacement transducers measured the vertical translation of the cylinder at about its midheight; however, the central cylinder is so rigid in the axial direction compared to the bending stiffness of the central disk that the measured vertical deformations can be taken to be the same along the length of the cylinder, and thus represent the deflection under the load. Measuring the displacements at three circumferential locations also provides an indication of the uniformity of the plate properties. Figure 8 shows a photograph of the test setup. The load was applied by a computer-controlled 600-kip servo-hydraulic actuator via a thick steel loading plate (see Fig. 5) in displacement control. The loading rate was 15 kips/min. Two load/unload cycles were applied to a peak load of 30 kips as shown in Figure 8.

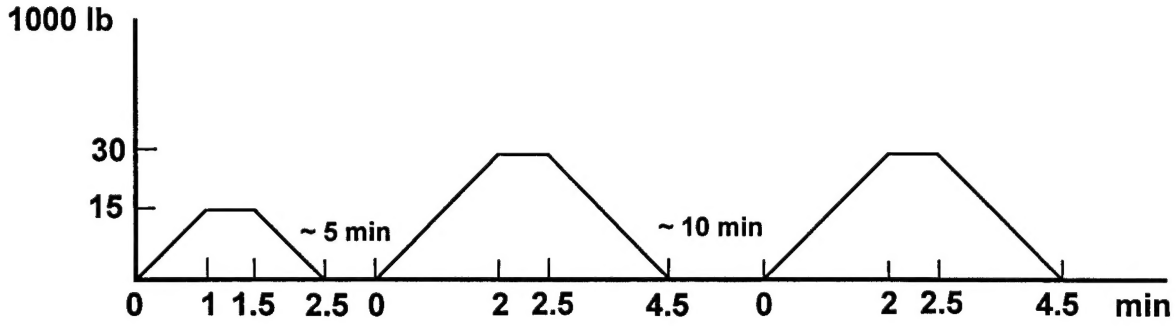

Figure 8. Loading sequence for static stiffness test of composite end plate.

The measured load-displacement curves are shown in Figure 9. The measurements show good agreement between the three gages, indicating uniform axisymmetric deflection. The deflection histories also show some hysteresis at both of the load levels. During the initial loading acoustic emissions were audible as the load was increased to 15 kips, and ceased upon unloading. No sounds were heard during reloading until the first load level of 15 kips was exceeded, then the sounds continued up to 30 kips, but decreased in frequency. The third repeat load cycle to 30 kips produced identical displacements and no sounds were audible. The acoustic emissions indicate resin microcracking that ceased with repeated loading. This behavior is not unusual for large RTM composite components loaded to significant load levels, and do not influence plate performance, as indicated by the repeatability of measured deflections during the load-unload cycles. The load deflection curves have a low stiffness toe that is the result of the slight nonplanarity of the center plate. The curves become linear, as would be expected, past about 10,000 lbs.

Analysis

A finite element analysis was performed to simulate the observed plate behavior. The plate was modeled with anisotropic, shear deformable shell elements for the composite components, and isotropic solid elements for the foam filling between the coil support and back support plates. The material properties used were those obtained from the coupon tests performed on the first plate [1] whenever available (measured), from micromechanics (calculated), or were estimated otherwise. The material properties used are shown in Table 1. The FEM model is shown in the figures that present the result. Only one-sixth of the plate was modeled with an alcove gusset at the center, since the loading and deformations are axisymmetric. Symmetry boundary conditions were applied at the

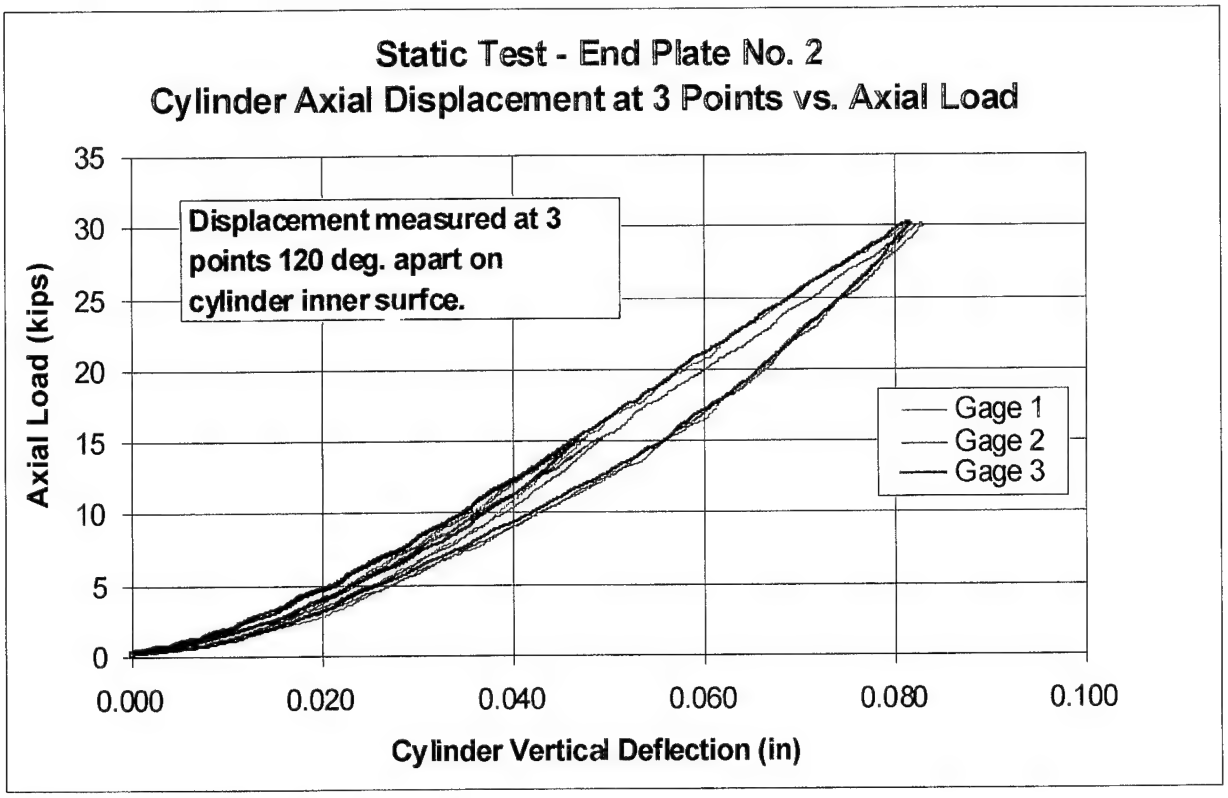

Figure 9. Load deflection curves for composite end plate.

lateral boundaries, and the model was constrained with simple supports at the location of the mounting hole center radius; the holes were not modeled. The loading and boundary conditions are shown in Figure 10. The results presented are for 6000 psi modulus isocyanate closed cell foam filling between the coil support ring and the center cylinder, as determined from manufacturer's data.

Table 1. Key Material Properties Used in FEM Calculations

Component x direction		Cylinder Axial	Plate radial	Alcove radial	Coil supp. axial	Foam fill N/A
Vf		0.4	0.55	0.51	0.55	-
Ex	(E6 psi)	4.220 e	6.450 m	5.234 c	5.803 m	0.0060 d
Ey	(E6 psi)	4.220 e	6.129 m	5.039 c	5.803 e	0.0060 d
Ez	(E6 psi)	1.000 e	1.000 e	1.000 e	1.000 c	0.0060 d
Gxy	(E6 psi)	0.710 e	2.000 c	1.793 c	0.710 e	0.0025 c
Nuxy		0.300 e	0.313 c	0.380 c	0.300 e	0.2000 d

m = measured
c = calculated
e = estimated
d = data supplied by manufacturer

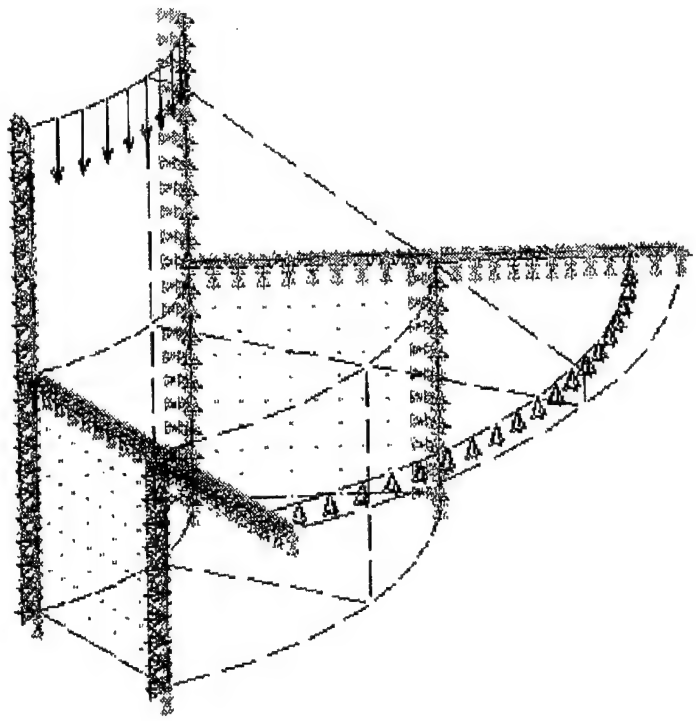

Figure 10. Loading and boundary conditions for end plate FEM analysis.

The deflection contours are shown in Figure 11, and the corresponding von Mises, maximum and minimum principal stresses (indicative of peak tensile and compressive stress magnitudes), and in-plane shear stresses are shown in Figures 12 through 15. The measured stiffness, in terms of center cylinder edge load and vertical deflection was calculated to be 425 kips/in. past the toe region. This compares favorably with the calculated stiffness of 375 kips/in., using E = 6000 psi for the foam insert, the difference being about 12%. Figure 16 shows the comparison of measured and calculated stiffnesses along with the load-deflection data. The difference between the measured and calculated stiffnesses is attributed to possible inaccuracies in the FEM model (for example, filleted radii were not modeled) and in some of the composite property data, particularly the in-plane and out-of-plane shear moduli. The properties used were conservative. The stress contours indicate stress concentration near the junction of the gussets and the inner cylinder. This stress state is consistent with the failure mode observed in the first end plate, as shown in Figure 17. The calculated stress levels are far below allowable everywhere. The measured and calculated stiffnesses compare favorably with the bending stiffness of the conventional titanium plate, which was estimated at 183 kips/in.

We note that the stiffness measurements did not simulate precisely the actual axial Lorentz loading on the end plate, but they give a qualitative indication of the performance of the plate. According to the original specifications, the axial Lorentz force was assumed to be 500 psi concentrated on a circular annulus with an inner radius of 11.7 in. (the outside radius of the coil support ring) and a width of 2.5 inches. The total Lorentz force then is 102,100 lbs. To put the test results in perspective, a flat plate analogy was used to compare the deflection of a flat circular annulus loaded with a concentrated ring load of 1250 lbs/in. at a radius of 13 inches (which is equivalent to the total Lorentz force) and a ring load applied at the radius of 7 inches on the central cylinder (as used in the static test). Figure 18 shows the analogy. Using a thickness of 1.0 inch and an "equivalent" plate modulus of 45×10^6 psi to capture the structural effects of the geometry, the

deflection of the plate was obtained at the inner edge. Ring loads of $F_1 = 102{,}100$ lbs and $F_2 = 28{,}100$ lbs give identical deflections of 0.088 inch (which is close to the value obtained by the FEM analysis for a load of $F_2 = 33{,}000$ lbs). This analogy indicates that the plate's load carrying capacity exceeds the loading requirements based on the axial Lorentz force.

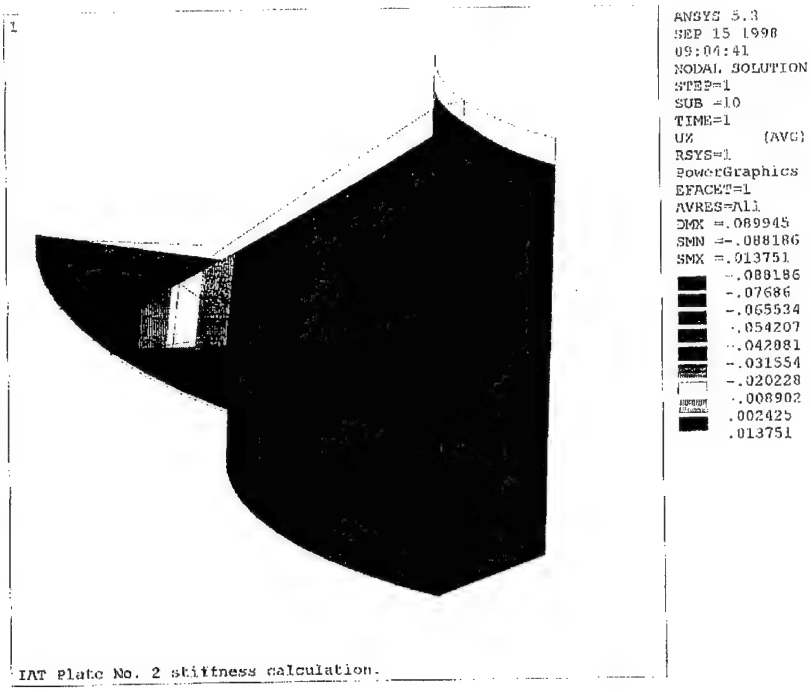

Figure 11. Axial displacement contours for composite end plate.

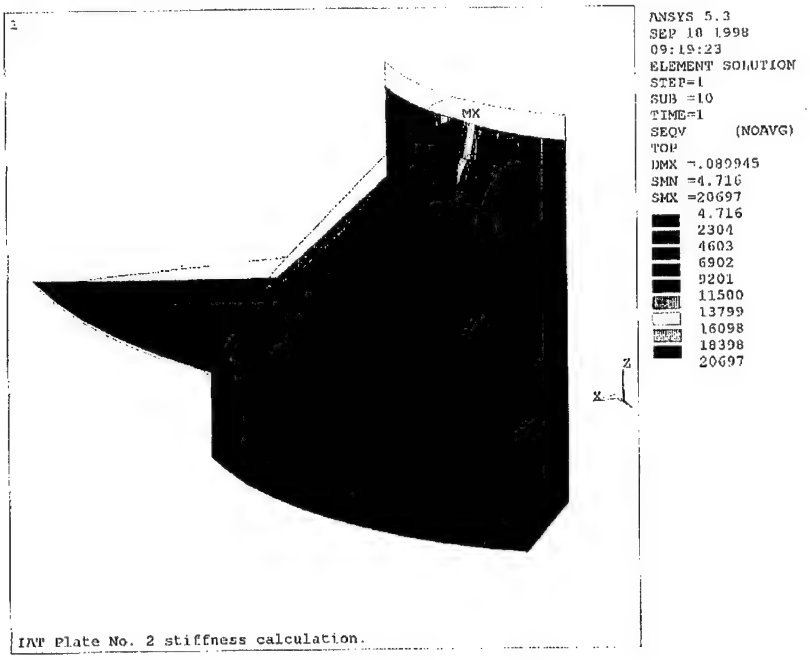

Figure 12. Von Mises stress contours for composite end plate.

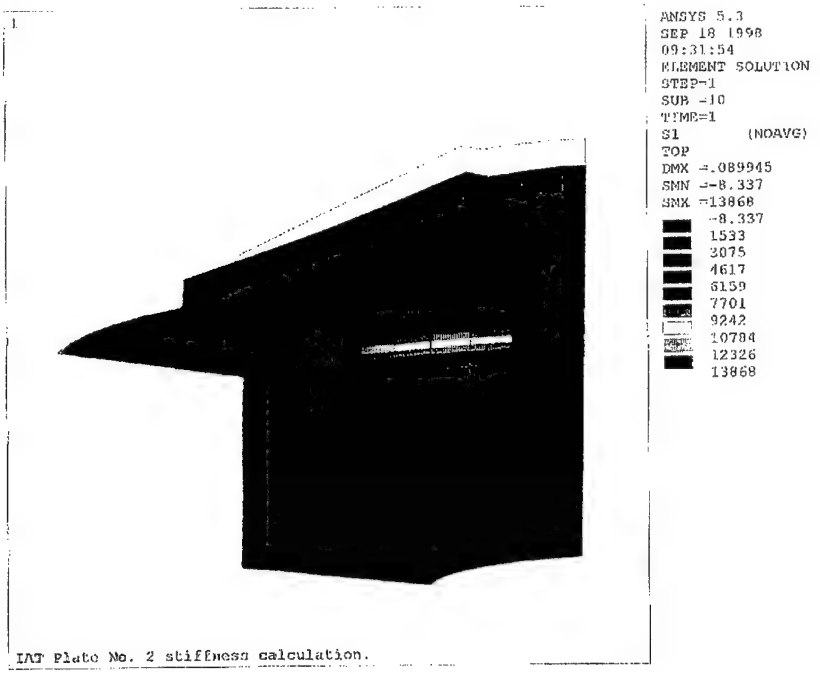

Figure 13. Major principal stress contours for composite end plate.

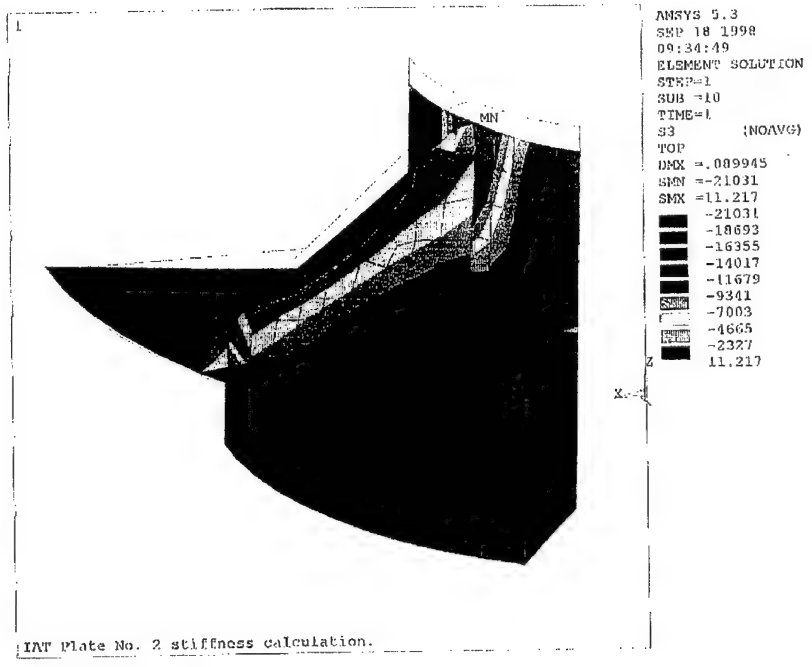

Figure 14. Minor principal stress contours for composite end plate.

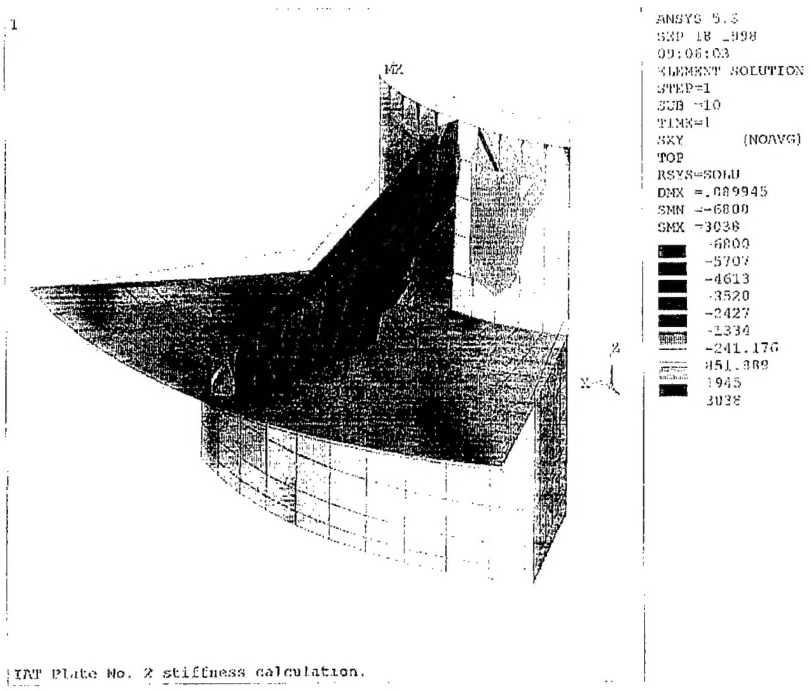

Figure 15. In-plane shear stress contours for composite end plate.

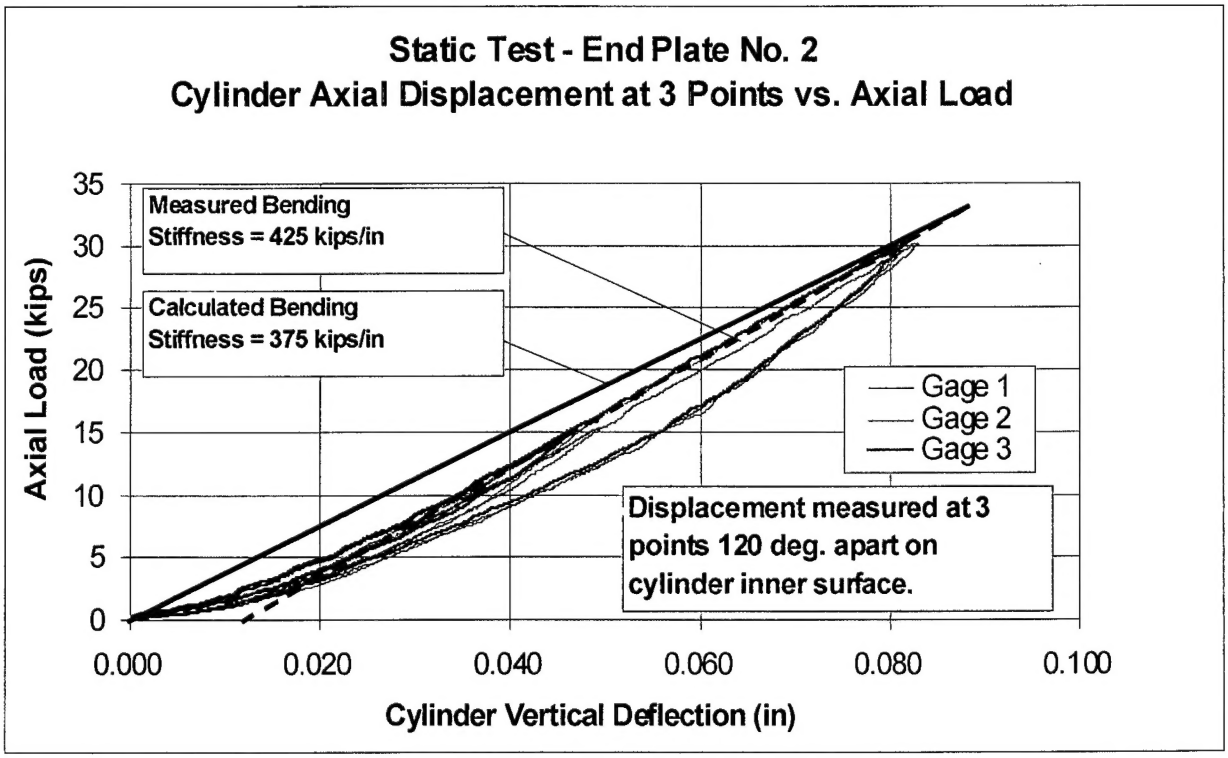

Figure 16. Load-deflection curves and measured and calculated stiffnesses for composite end plate.

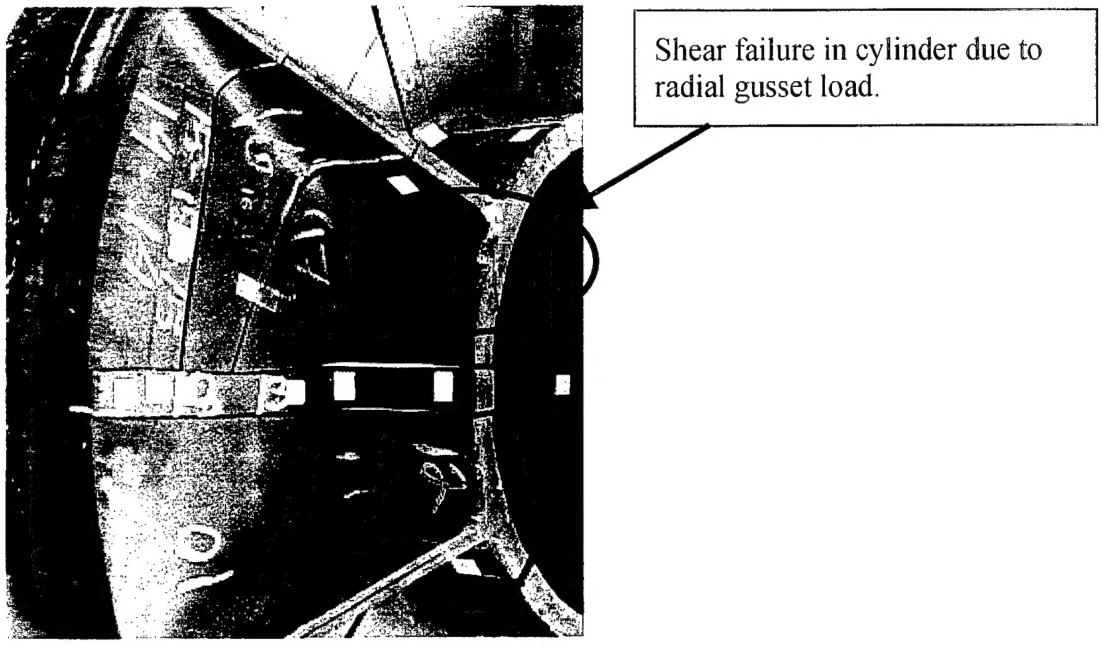

Figure 17. Typical shear failure in cylinder of first end plate due to radial gusset load.

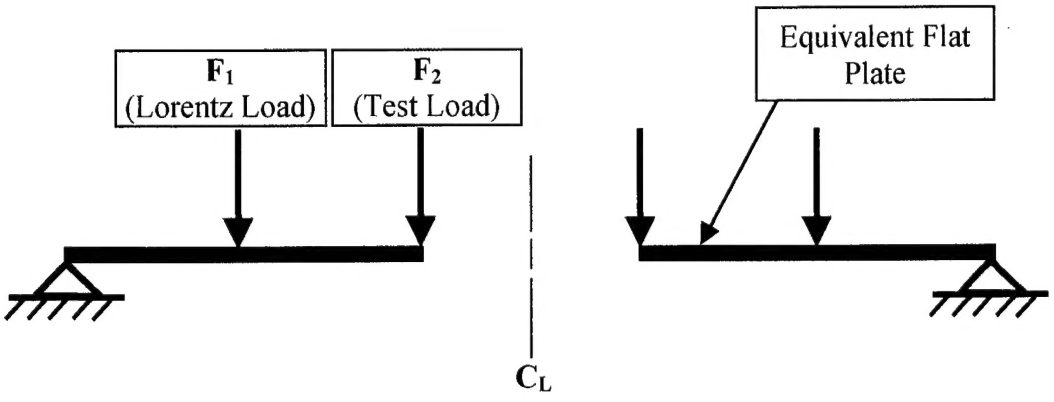

Figure 18. Flat plate analogy for static stiffness test.

Summary

The second carbon composite end plate was produced with the RTM process. The plate showed good overall quality and was machined to final dimension and tested statically to determine its structural stiffness. Static stiffness measurements were conducted up to load levels that were near the anticipated service load of the end plate with no deterioration in stiffness or inelastic behavior. Finite element calculations, using measured and calculated properties, were done to simulate the static test, and calculated and measured axial stiffnesses were within 12%. The completed plate was sent to the University of Texas for evaluation and testing.

Acknowledgment

This work was supported by the U.S. Army Research Laboratory (ARL) under contract DAAA21-93-C-0101.

References

[1] DR Technologies, "Fabrication and Testing of the First RTM Carbon Fiber Composite End Plate," Interim Report, UT/IAT Subcontract No. UTA96-0098, September 1997.

Distribution List

Administrator
Defense Technical Information Center
Attn: DTIC-DDA
8725 John J. Kingman Road,
Ste 0944
Ft. Belvoir, VA 22060-6218

Director
US Army Research Lab
ATTN: AMSRL OP SD TA
2800 Powder Mill Road
Adelphi, MD 20783-1145

Director
US Army Research Lab
ATTN: AMSRL OP SD TL
2800 Powder Mill Road
Adelphi, MD 20783-1145

Director
US Army Research Lab
ATTN: AMSRL OP SD TP
2800 Powder Mill Road
Adelphi, MD 20783-1145

Army Research Laboratory
AMSRL-CI-LP
Technical Library 305
Aberdeen Prvg Grd, MD 21005-5066

Dr. Bruce Burns
U.S Army Research Laboratory
Attn: AMSRL-WT-PD
Bldg. 390
Aberdeen Prvg Grd, MD 21005-5066

Dr. Dan Dakin
Science Applications International Corp.
2000 Powell St., Suite 1090
Emeryville, CA 94608

Dr. Donald Eccleshall
Institute for Advanced Technology
The University of Texas at Austin
4030-2 W. Braker Lane
Austin, TX 78759

Dr. Marilyn Freeman
DARPA/TTO
3701 N. Fairfax Drive
Arlington, VA 22203-1714

Dr. Thaddeus Gora
U.S. Army Armament Research,
Development and Engineering Center
Attn: AMSTA-AR-FS Bldg. 94
Picatinny Arsenal, NJ 07806-5000

Dr. Walter LaBerge
Institute for Advanced Technology
The University of Texas at Austin
4030-2 West Braker Lane
Austin, TX 78759

Mr. Dennis Ladd
Commander, TACOM-ARDEC
Attn: AMSTA-AR-FSP-E / Dennis Ladd
Bldg. 354
Picatinny Arsenal, NJ 07806-5000

Dr. Andrus Niiler
U.S. Army Research Laboratory
Attn: AMSRL-WM-TA
Aberdeen Prvg Grd, MD 21005-5066

Dr. William Rienstra
8200 N. Mopac Suite #150
Mailbox 14
Austin, TX 78759

Dr. Stuart N. Rosenwasser
DR Technologies, Inc.
11585 Sorrento Valley Road
Suite 103
San Diego, CA 92121

Mr. D. W. Scherbarth
Westinghouse Electric Corporation
Science and Technology Center
1310 Beulah Road
Pittsburgh, PA 15235

Dr. Edward M. Schmidt
U.S. Army Research Laboratory
Attn: AMSRL-WT-B
Aberdeen Prvg Grd, MD 21005-5066

Dr. Jerome T. Tzeng
U.S. Army Research Laboratory
Weapons Technology Directorate
ATTN: AMSRL-WT-PD
APG, MD 21005

Mr. Alan Walls
Center for Electromechanics
The University of Texas at Austin
PRC, Mail Code R7000
Austin, TX 78712